Enhancement of the photo conversion efficiencies in Cu(In,Ga)(Se,S)2 solar cells fabricated by two-step sulfurization process

JungYup Yang, Junggyu Nam, Dongseop Kim, GeeYeong Kim, William Jo, Yoonmook Kang, and Dongho Lee

Citation: Applied Physics Letters **107**, 193901 (2015); doi: 10.1063/1.4935333
View online: http://dx.doi.org/10.1063/1.4935333
View Table of Contents: http://scitation.aip.org/content/aip/journal/apl/107/19?ver=pdfcov
Published by the AIP Publishing

Enhancement of the photo conversion efficiencies in Cu(In,Ga)(Se,S)$_2$ solar cells fabricated by two-step sulfurization process

JungYup Yang,[1] Junggyu Nam,[1] Dongseop Kim,[1] GeeYeong Kim,[2] William Jo,[2] Yoonmook Kang,[3,a)] and Dongho Lee[1,a)]
[1]*Photovoltaic Development Team, Energy Storage Business Division, Samsung SDI, Cheonan-si 331-300, South Korea*
[2]*Department of Physics and New and Renewable Energy Research Center, Ewha Womans University, Seoul 120-750, South Korea*
[3]*KUKIST Green School, Graduate School of Energy and Environment, Korea University, Seoul 136-701, South Korea*

(Received 6 September 2015; accepted 26 October 2015; published online 9 November 2015)

Cu(In,Ga)(Se,S)$_2$ (CIGSS) absorber layers were fabricated by using a modified two-stage sputter and a sequential selenization/sulfurization method, and the sulfurization process is changed from one-step to two-step. The two-step sulfurization was controlled with two different H_2S gas concentrations during the sulfurization treatment. This two-step process yielded remarkable improvements in the efficiency (+0.7%), open circuit voltage (+14 mV), short circuit current (+0.23 mA/cm^2), and fill factor (+0.21%) of a CIGSS device with 30×30 cm^2 in size, owing to the good passivation at the grain boundary surface, uniform material composition among the grain boundaries, and modified depth profile of Ga and S. The deterioration of the P/N junction quality was prevented by the optimized S content in the CIGSS absorber layer. The effects of the passivation quality at the grain boundary surface, the material uniformity, the compositional depth profiles, the microstructure, and the electrical characteristics were examined by Kelvin probe force microscopy, X-ray diffraction, secondary ion mass spectrometry, scanning electron microscopy, and current-voltage curves, respectively. The two-step sulfurization process is experimentally found to be useful for obtaining good surface conditions and, enhancing the efficiency, for the mass production of large CIGSS modules. © *2015 AIP Publishing LLC*. [http://dx.doi.org/10.1063/1.4935333]

Thin-film photovoltaic (PV) technologies entered the market only in recent years and have great potential.[1] Thin-film productions use only a small amount of materials compared with wafer-based silicon devices and enable the integrated production of interconnected modules. Furthermore, Cu(In,Ga)Se$_2$ (CIGSe) based thin-film solar cells recently exhibited power conversion efficiencies over 20% in laboratory tests.[2–5] A recent work reported the highest efficiency of 21.7% using a three-stage co-evaporation method.[5] This efficiency of 21.7% is highly significant, as the CIGSe solar cells exhibit a higher efficiency than multi-crystalline silicon solar cells. However, the applicability of this approach for the mass production of large scale CIGSe films is limited by the low throughput and poor film uniformity. The sputtering and sequential selenization/sulfurization process is employed in mass production because of the advantages of the throughput and the uniformity of large sized modules.[6]

We performed several research projects to increase the Cu(In,Ga)(Se,Se)$_2$ (CIGSS) module efficiency by improving the quality of the CIGSS absorber. One of the major projects involved the high temperature sulfurization process. Devices prepared by this process exhibited an increase in the open circuit voltage (V_{oc}) and short circuit current density (J_{sc}), owing to the improvements in the grain quality and the band-gap (E_g) grading. However, in the high temperature furnace process using a large glass substrate, the sulfur profile cannot be precisely controlled, because of the very fast sulfur reaction at a high temperature with a long process time.[7–9] Moreover, shortening the sulfurization process to optimize the sulfur profile has resulted in the poor uniformity of the CIGSS absorber layer. In this letter, we propose a two-step sulfurization method for the first time, wherein the H_2S gas concentration is changed during the sulfurization process in order to eliminate the negative effects of the sulfurization and improve the quality of the CIGSS absorber layer. The detailed structure and optical and electronic properties are discussed with respect to the two-step sulfurization process.

$Cu_{0.72}Ga_{0.28}$ and In were deposited by DC sputtering on a 300 nm thick Mo back electrode and also by using a sputtering system on a cleaned high strain point glass at room temperature. The Cu/(Ga + In) composition was controlled according to the film thickness and fixed at ~0.87. CIGSS absorber layers with a thickness of ~1.6 μm were formed through a reaction of the CuGa/In precursors with H_2Se and H_2S gases. Figure 1(a) shows the temperature profile of the typical CIGSS absorber formation comprising a conventional two-stage process. In the first stage, a graded band-gap CIGSe absorber was fabricated intentionally by the selenization of the metal precursors in the H_2Se gas atmosphere. In the second stage, a thin CIGSS surface layer was formed on the CIGSe absorber surface by sulfurization with H_2S gas to prepare a double graded band-gap profile. In the conventional two-stage sputtering and selenization/sulfurization process, a long time and high temperature profile for the sulfurization is required to uniformly diffuse Ga because the

a)Authors to whom correspondence should be addressed. Electronic addresses: dhlee0333@gmail.com and ddang@korea.ac.kr

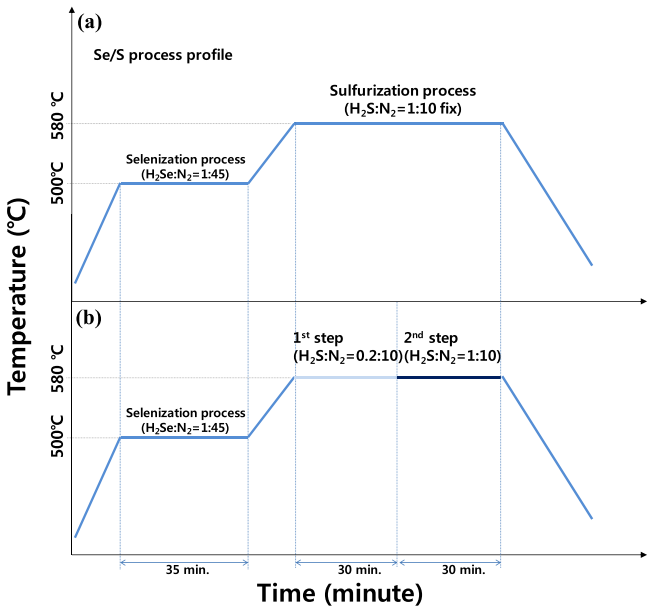

FIG. 1. Temperature profiles of two-stage selenization/sulfurization process. (a) Baseline one-step sulfurization process and (b) optimized two-step sulfurization process.

diffusivity of Ga is substantially lower than that of other elements. However, it is difficult to obtain a high efficiency using the typical one-step sulfurization process at a high temperature, despite numerous attempts to increase the efficiency because of the harmful effects of the strong sulfurization.[7,10] Figure 1(b) shows the optimized process profile of the two-step sulfurization process, where the second stage was modified by changing the H_2S gas concentrations during the sulfurization. This first and second sulfurization steps were performed at low and high H_2S gas concentrations, respectively. The two-step sulfurization process employs two-step H_2S gas concentrations during the sulfurization for preventing over-sulfurization and improving the device performance.

Heterojunctions were formed by the chemical bath deposition of ~5 nm of a Zn(O,OH,S) buffer layer, and then boron-doped ZnO was deposited on the buffer layer as a transparent conducting oxide top contact layer using low-pressure chemical vapor deposition. One laser (P1) and two mechanical (P2 and P3) scribing techniques were applied to form a monolithic interconnection. The morphologies and microstructure of the absorber layer were measured by scanning electron microscopy (SEM). Secondary ion mass spectrometry (SIMS) was used to detect the compositional depth profiles in the CIGSS absorber layers. The solar cell performance was characterized by current versus voltage (I-V) measurements under AM1.5, 100 mW/cm^2 illumination at 25 °C. The fill factor (FF), efficiency (Eff), V_{oc}, and short-circuit current density (J_{sc}) were extracted from the I-V curves. The series resistance (R_s), shunt resistance (R_{sh}), and diode ideality factor (N-factor) were calculated using the sunshade method.[11] The optical response characteristics of the solar cell were measured according to the external quantum efficiency (EQE). The bulk and surface crystal structures were studied by X-ray diffraction (XRD) and grazing incidence XRD (GIXRD), respectively. The surface work-function and potential distributions at the grain boundaries in the CIGSS absorber layer were measured by Kelvin probe force microscopy (KPFM) using a commercial atomic force microscope. KPFM measurements performed in this study are described in detail elsewhere.[12,13]

Figure 2(a) shows the sunshade I-V characteristics of a 30×30 cm^2 monolithic module (defined as comprising of a series connected CIGSS cells before lamination) having 64 series-connected cells with an aperture area of 878.6 cm^2 that were fabricated by one and two-step sulfurization processes. The corresponding Eff, V_{oc}, J_{sc}, FF, R_s, R_{sh}, N-factor, E_g, and reverse saturation current (J_0) are presented in Table I. As shown in Fig. 2(a) and Table I, all the device parameters were clearly enhanced for the two-step sulfurization process, including Eff + 0.7%, V_{oc} + 14 mV, J_{sc} + 0.23 mA/cm^2, and FF + 0.21%. It is attributed to the improvement of the device parameters to optimized sulfur profile into CIGSS absorber layer and improved bulk and surface quality of absorber layer by applying two-step sulfurization process. The influence of the one and two-step sulfurization on the electronic properties of the junctions is more clearly observed by analyzing the EQE of the samples. Figure 2(b) presents normalized EQE curves of the solar cells with absorbers manufactured by the two-step (red circuit) and one-step (black square) sulfurization processes. Here, the EQE curve of the one-step devices is

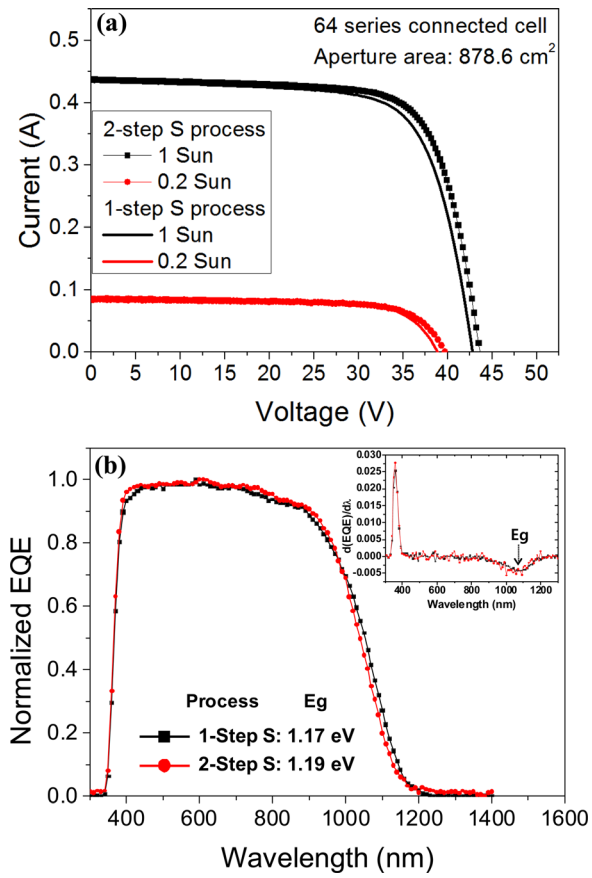

FIG. 2. (a) I-V characteristics (black line: 1 sun, red line: 0.2 sun) of the 300×300 mm^2 sized CIGSS monolithic module made by the one-step (line) and two-step (symbol line) sulfurization processes. The R_s, R_{sh}, and N-factor were calculated by the sunshade method. (b) The normalized EQE curve of the CIGSS absorber layer fabricated by one-step and two-step sulfurization processes. The inset figure shows the d(QE)/dλ curve as a function of the wavelength, which is used to determine E_g.

TABLE I. CIGSS device characteristics were fabricated by one- and two-step sulfurization processes. The device parameters: Eff, V_{oc}, J_{sc}, R_s, R_{sh}, FF, N-factor, E_g, and J_0 are listed.

Process	Eff (%)	V_{oc} (V)	J_{sc} (mA/cm^2)	FF (%)	R_s (Ω cm^2)	R_{sh} (Ω cm^2)	N-factor	E_g (eV)	J_0 (A/cm^2)
One-step sulfurization process	15.15	0.669	31.63	71.62	1.26	1225	1.50	1.17	7.9×10^{-10}
Two-step sulfurization process	15.85	0.683	31.86	72.83	1.19	1473	1.47	1.19	3.2×10^{-10}

lower than that of the two-step sample. This clearly indicates that the two-step device exhibits better quantum efficiency because of the higher absorber bulk and interface quality of the two-step CIGSS layer compared with the one-step CIGSS layer. The inset in Fig. 2(b) shows the E_g, which was determined by the differentiation of EQE curve and used to obtain the E_g values precisely. The E_g of the CIGSS absorber layer fabricated by one- and two-step sulfurization processes was 1.17 eV and 1.19 eV, respectively.

Figure 3 shows the Ga/(In + Ga) (GGI) ratio and S/(Se + S) (SSSe) ratio with respect to the CIGSS absorber layer thickness measured by SIMS for different sulfurization processes. The closed and open symbols indicate one- and two-step sulfurization data, respectively. The S/(Se + S) profile shows the decrease over the whole CIGSS absorber layer without changing the Ga/(In + Ga) profile under the two-step sulfurization process, as shown in Fig. 3. It is well-known that Ga diffusion typically occurs during sulfurization process in two-stage sputter and selenization/sulfurization method because the sulfurization requires higher temperature than the selenization.[7] In our case, the lack of a difference in the Ga/(In + Ga) profile between the one- and two-step sulfurization is probably related to the identical thermal budget due to the equal process temperature and time among the two methods. Therefore, it is possible to increase the absorber bulk and interface quality through the precise-control of the sulfur content in the CIGSS absorber layer by the two-step sulfurization process as well as to obtain the similar grain size of the CIGSS absorber layer with a similar GGI profile. The microstructure grain images measured by SEM are shown in Fig. S1.[14]

The surface properties of the CIGSS absorber were investigated by KPFM because the sulfurization process influences the surface quality of the absorber layer. The surface work-function and surface potential distribution on the CIGSS absorber layer can be obtained through a KPFM measurement, whereby the contact potential difference (V_{CPD}) between a conducting AFM tip and the sample is determined. We measured the tip work function using highly ordered pyrolytic graphite. The V_{CPD} between the tip and sample is defined as $V_{CPD} = (\phi_{tip} - \phi_{sample})/-e$, where ϕ_{sample} and ϕ_{tip} are the work-functions of the sample and tip, respectively, and e is the electric charge. This method is described in detail elsewhere.[13,15] Figure 4 shows the KPFM results for CIGSS absorber layers fabricated by different sulfurization processes. In Fig. 4(a), the black and pink squares indicate the one- and two-step sulfurization processes, respectively. Generally, the value of the CIGSS work function is 4.5–5.5 eV.[16] As shown in Fig. 4(a), the

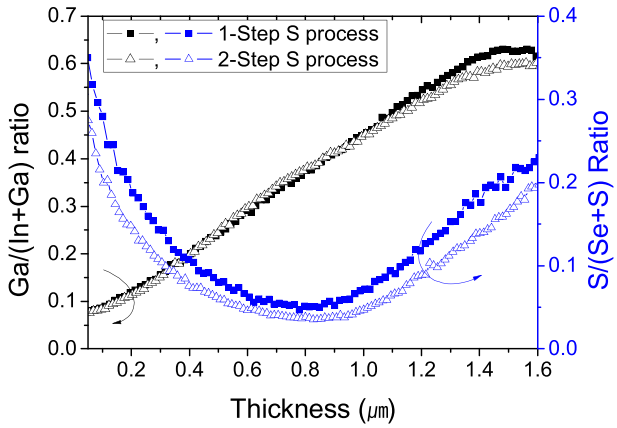

FIG. 3. (a) Ga/(Ga + In) and (b) S/(S + Se) SIMS profiles of CIGSS absorber layers fabricated by one-step (square) and two-step (triangle) sulfurization processes.

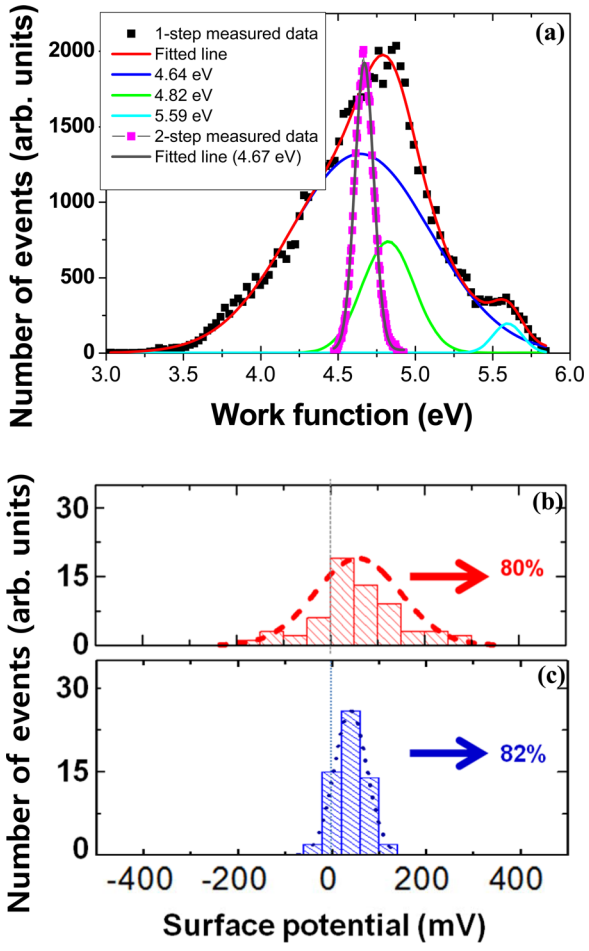

FIG. 4. KPFM results for the CIGSS absorber layer with different sulfurization processes: (a) Work-function distribution, (b) and (c) the statistical surface potential distribution at the grain boundaries of the CIGSS absorber layer fabricated by the one- and two-step sulfurization processes, respectively.

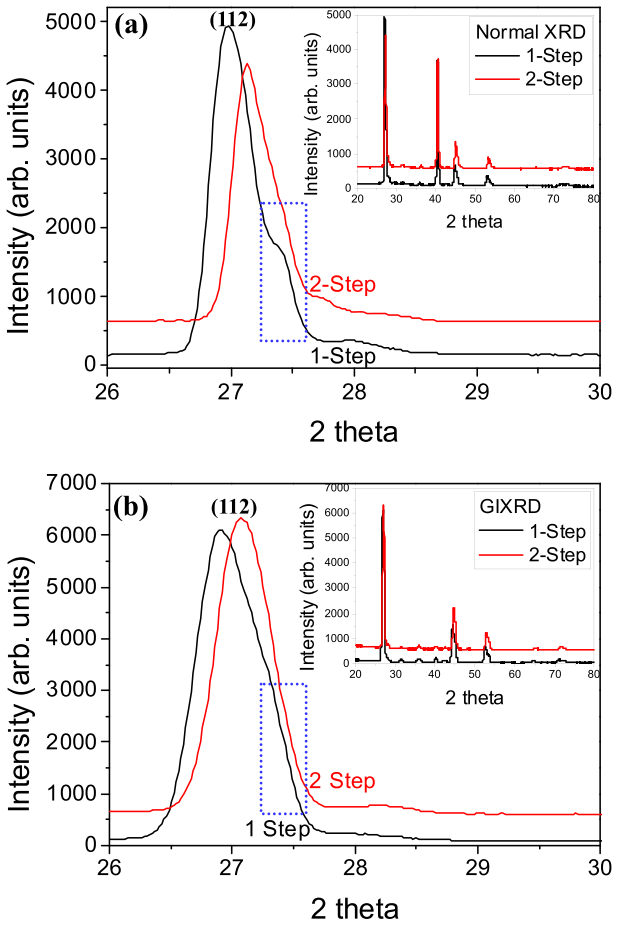

FIG. 5. Enlarged (a) XRD and (b) GIXRD results for the CIGSS absorber layer fabricated by the one- and two-step sulfurization processes. The inset figures show the overall range of the measured XRD and GIXRD data.

work-function distributions on the CIGSS surface fabricated by the two-step sulfurization process are sharp when compared with those for the one-step sulfurization process. This means that the surface state in the CIGSS absorber fabricated by the two-step sulfurization temperature was more uniform than that of the CIGSS absorber treated with one-step sulfurization.

Figures 4(b) and 4(c) show statistical potential distributions based on the KPFM results for the CIGSS absorber surface focusing on grain boundaries fabricated by the one- and two-step sulfurization processes, respectively. The positive potential distributions at the grain boundaries can enhance the device performance because the surface energy band at the grain boundaries is bent by the positive potential at the grain boundaries. The bent energy band plays an important role in the passivation at grain boundaries.[12,17,18] As shown in Figs. 4(b) and 4(c), the potential distributions at the grain boundaries of the CIGSS absorber layer fabricated by the two-step process exhibit larger positive values than those for the one-step process. Thus, the two-step sulfurization process enhanced not only the uniformity of materials at the absorber layer surface but also the passivation property at the grain boundaries. In the first sulfurization step, the grain size of the absorber material was improved by using low a concentration H_2S gas, which diffused into the grain boundaries during the second sulfurization step. If the first sulfurization step is performed under an inert gas condition (such as N_2 or Ar gas), many voids form across the CIGSS film. Therefore, we used a low concentration of the H_2S gas in the first sulfurization step.

To analyze the CIGSS surface and bulk microstructure in detail, we investigated the bulk and surface crystallization using XRD. Figures 5(a) and 5(b) present CuKα two-theta XRD and GIXRD patterns of the CIGSS absorber layer fabricated by one- and two-step sulfurization processes, respectively. The overall range XRD and GIXRD spectra of the CIGSS absorber are shown in the insets. As shown in Figs. 5(a) and 5(b), the CIGSS absorber film fabricated by the two-step sulfurization exhibited a decrease in the shoulder peak (about 27.5°, as indicated by blue box) at the high-angle side of the (112) main diffraction for the CIGSS layer owing to the improvement in the homogeneity for material compositions between the grains in the overall CIGSS absorber layer from surface to bulk.

In conclusion, we investigated the interface states and bulk quality of CIGSS absorber layers in order to optimize the sulfurization process in CIGSS absorber layers fabricated by a two-stage sputtering and selenization/sulfurization method. For the optimization of the sulfur profile in the CIGSS absorber layer, we propose a method of two-step sulfurization, wherein the H_2S gas concentration is changed during the sulfurization process. Using the two-step sulfurization process, we achieved an efficiency of 15.85%, which is 0.7% higher than that obtained using the conventional one-step sulfurization process. This two-step sulfurization process was experimentally demonstrated to be useful for enhancing the efficiency of CIGSS solar cells and for the mass production of large sized CIGSS modules.

This work was supported by the New & Renewable Energy Core Technology Program of the Korea Institute of Energy Technology Evaluation and Planning (KETEP) and was granted financial resource from the Ministry of Trade, Industry & Energy, Republic of Korea (No. 20143030011960) and by the National Research Foundation of Korea, grant funded by the Korean Government (MSIP) (2015, University-Institute cooperation program).

[1]A. Shah, P. Torres, R. Tscharner, N. Wyrsch, and H. Keppner, "Photovoltaic technology: The case for thin-film solar cells," Science **285**, 692 (1999).
[2]M. A. Green, K. Emery, Y. Hishikawa, W. Warta, and E. D. Dunlop, "Solar cell efficiency tables (version 44)," Prog. Photovoltaics Res. Appl. **22**, 701 (2014).
[3]P. Jackson, D. Hariskos, R. Wuerz, W. Wischmann, and M. Powalla, "Compositional investigation of potassium doped Cu(In,Ga)Se_2 solar cells with efficiencies up to 20.8%," Phys. Status Solidi (RRL) **8**(3), 219 (2014).
[4]A. Chirila, P. Reinhard, F. Pianezzi, P. Bloesch, A. R. Uhl, C. Fella, L. Kranz, D. Keller, C. Gretener, H. Hagendorfer *et al.*, "Potassium-induced surface modification of Cu(In,Ga)Se_2 thin films for high-efficiency solar cells," Nat. Mater. **12**, 1107 (2013).
[5]P. Jackson, D. Hariskos, R. Wuerz, O. Kiowski, A. Bauer, T. M. Friedlmeier, and M. Powalla, Phys. Status Solidi (RRL) **9**, 28 (2015).
[6]T.-T. Wu, J.-H. Huang, F. Hu, C.-H. Chang, W.-L. Liu, T.-H. Wang, C.-H. Shen, J.-M. Shieh, and Y.-L. Chueh, Nano Energy **10**, 28 (2014).
[7]Y. Goushi, H. Hakuma, K. Tabuchi, S. Kijima, and K. Kushiya, Sol. Energy Mater. Sol. Cells **93**, 1318 (2009).
[8]R. Knecht, M. S. Hammer, J. Parisi, and I. Riedel, Phys. Status Solidi A **210**, 1392 (2013).
[9]T. Nakada, H. Ohbo, T. Watanabe, H. Nakazawa, M. Matsui, and A. Kunioka, Sol. Energy Mater. Sol. Cells **49**, 285 (1997).
[10]K. Kushiya, Sol. Energy Mater. Sol. Cells **93**, 1037 (2009).

[11]S. Bowden and A. Rohatgi, in *Proceedings of 17th European Photovoltaic Solar Energy Conference*, 2001, p. 1802.
[12]G. Y. Kim, A. R. Jeong, J. R. Kim, W. Jo, D.-H. Son, D.-H. Kim, and J.-K. Kang, Sol. Energy Mater. Sol. Cells **127**, 129 (2014).
[13]W. Melitz, J. Shen, A. C. Kummel, and S. Lee, Surf. Sci. Rep. **66**, 1 (2011).
[14]See supplementary material at http://dx.doi.org/10.1063/1.4935333 for SEM microstructure images.
[15]C.-S. Jiang, R. Nou, K. Ramanathan, J. A. AbuShama, H. R. Moutinho, and M. M. Al-Jassim, Appl. Phys. Lett. **85**, 2625 (2004).
[16]R. Baier, J. Lehmann, S. Lehmann, T. Rissom, C. A. Kaufmann, A. Schwarzmann, Y. Rosenwaks, M. Ch. Lux-Steiner, and S. Sadewasser, Sol. Energy Mater. Sol. Cells **103**, 86 (2012).
[17]J. B. Li, V. Chawla, and B. M. Clemens, Adv. Mater. **24**, 720 (2012).
[18]M. Hafemeister, S. Siebentritt, J. Albert, M. C. Lux-Steiner, and S. Sadewasser, Phys. Rev. Lett. **104**, 196602 (2010).